# Control of centrifugal fingering via a variable interfacial tension approach

Francisco M. Rocha and José A. Miranda*
*Departamento de Física, Universidade Federal de Pernambuco, Recife, Pernambuco 50670-901, Brazil*
(Received 20 August 2013; published 17 September 2013)

We study the centrifugal fingering instabilities that occur in rotating Hele-Shaw cells containing two different fluids. A weakly nonlinear analysis of the problem is performed, considering that the surface tension between the rotating fluids changes with the local curvature of the interface. It is shown that the coupling between the contact angle and the variable interfacial tension permits the control of the interface disturbances. As a result, linear perturbations and nonlinear finger competition phenomena can be properly controlled and suppressed.

DOI: 10.1103/PhysRevE.88.033008 PACS number(s): 47.15.gp, 47.20.Ma, 47.55.N−, 47.54.−r

## I. INTRODUCTION

It is well known that the Saffman-Taylor instability [1] takes place in the confined geometry of motionless Hele-Shaw cells, being generated by the viscosity difference between the moving fluids (viscosity-driven instability). If the less viscous fluid pushes the more viscous one the interface is unstable, and patterned structures presenting multiple fingertip splitting are formed. However, if the more viscous fluid displaces the less viscous one (reverse viscous flow), the system is stable and no interfacial instability is observed [2].

A different kind of instability occurs if the Hele-Shaw cell is allowed to rotate with constant angular velocity around a vertical axis that passes through its center [3]. In this rotating version of the problem, the fluid-fluid interface may become unstable even under reverse viscous flow, due to the density difference between the fluids. This characterizes a centrifugally driven hydrodynamic instability [4–10]. If the inner fluid is denser, centrifugal viscous fingering arise, leading to the formation of interfacial patterns that are very distinct from those obtained in the usual viscosity-driven case. Instead of presenting branched, tip-split fingers, the rotating patterns exhibit fingers of different lengths, which compete with each other.

Rotating Hele-Shaw flows have been the object of considerable interest during the past two decades [11]. Among other things, this particular type of rotating flow has been serving as a useful prototypical system, with relevance to the modeling of biological systems involving tissue growth in rotating bioreactors [12], cell spreading [13], and cell motility [14]. It is also related to the technological problem of spin coating [15,16], which involves the rotation of thin fluid films in low-dimensional environments. On the theoretical side, researchers have been giving continued attention to rigorous exact solutions of fluid flows in such confined rotating systems [17–21].

Despite the significant number of studies examining the occurrence of interfacial instabilities and complex patterns in rotating Hele-Shaw cells, and other confined centrifugally driven systems, there are situations in which the formation of interfacial irregularities is undesirable. For example, in rotating bioreactors [12] and spin coating processes [15,16] the emergence of centrifugally driven instabilities can result in uneven or defective surface coverage. Therefore, it is of both academic and practical importance to find ways to control the growth of interfacial disturbances in this class of rotating flow problems.

As a matter of fact, the development of controlling strategies to the usual viscosity-driven viscous fingering problem has been a topic of major recent interest [22–31]. One particularly simple and efficient controlling method has been proposed in Ref. [31] which considers a curvature-dependent surface-tension model [32,33]. Within the context of this model, the surface tension varies in proportion to the local curvature of the evolving interface [34]. This strategy allowed the manipulation of the conventional viscosity-driven Saffman-Taylor instability leading to the suppression of fingertip-splitting events, and ultimate stabilization of the deformed interface.

Motivated by the success of the variable interfacial tension approach in controlling the usual viscosity-driven instability in motionless radial Hele-Shaw cells [31], in this work we investigate the possibility of restraining the emergence of centrifugal viscous fingering instability in rotating Hele-Shaw flows. Through the employment of a weakly nonlinear perturbative scheme [35] we show that the interplay between the variable surface tension and three-dimensional (3D) effects connected to the contact angle significantly affects the scenario of instability formation. The effectiveness of our controlling protocol is examined at both linear and early nonlinear stages of the dynamics, indicating inhibition of finger competition phenomena, and consequent stabilization of the rotating fluid-fluid interface.

## II. GOVERNING EQUATIONS OF THE PROBLEM

Consider a Hele-Shaw cell of gap spacing $b$ containing two immiscible, incompressible, viscous fluids (Fig. 1). Denote the densities and viscosities of the inner and outer fluids, respectively as $\rho_1, \eta_1$ and $\rho_2, \eta_2$. Although our model is capable of describing two fluids of densities and viscosities of any magnitude, we focus on the centrifugally driven motion where $\rho_1 > \rho_2$, and $\eta_1 \gg \eta_2$. The cell rotates with constant angular velocity $\Omega$, and there exists a surface tension $\sigma$ between the fluids. As in Refs. [31–33] the interfacial tension is not constant, and varies along the fluid-fluid interface.

To perform the weakly nonlinear analysis of the system, we consider that the initial circular fluid-fluid interface is slightly perturbed (Fig. 1), $\mathfrak{R} = R + \zeta(\theta,t)$, where $\theta$ represents the azimuthal angle and $R$ is the radius of the initially

*jme@df.ufpe.br

 

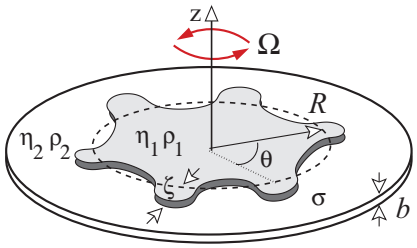


FIG. 1. (Color online) Perspective view of the rotating Hele-Shaw cell. The plates of the cell have spacing $b$ and rotate about a perpendicular $z$ axis with angular velocity $\Omega$. The more viscous and more dense fluid has initial radius $R$ and occupies the shaded region. Interface disturbances are denoted by $\zeta$, azimuthal angle by $\theta$, and the variable interfacial tension between the fluids is given by $\sigma$.

circular interface. The interface perturbation is written in the form of a Fourier expansion $\zeta(\theta,t) = \sum_{n=-\infty}^{+\infty} \zeta_n(t) \exp(in\theta)$, where $\zeta/R \ll 1$, $\zeta_n(t) = (1/2\pi)\int_0^{2\pi} \zeta(\theta,t)\exp(-in\theta)\mathrm{d}\theta$ denotes the complex Fourier mode amplitudes, and $n$ is an integer wave number.

The $n = 0$ mode is included in our analysis to keep the area of the perturbed shape independent of the perturbation $\zeta$. Mass conservation imposes that the zeroth mode is written in terms of the other modes as $\zeta_0 = -(1/2R)\sum_{n\neq 0} |\zeta_n(t)|^2$. Note that in order to address both linear and weakly nonlinear aspects of the interface dynamics, our perturbative analysis keeps terms up to the second order in $\zeta$.

The equation of motion of the interface is given by Darcy's law [1,2], properly augmented by a centrifugally driven term [3,4]

$$\mathbf{v}_j = -\frac{b^2}{12\eta_j}\nabla\left[p_j - \frac{\rho_j\Omega^2 r^2}{2}\right], \tag{1}$$

where $\mathbf{v}_j$ and $p_j$ represent the gap-averaged velocity and pressure of fluid $j$, where $j = 1,2$. In addition, $r$ denotes the radial distance from the axis of rotation. Equation (1) is valid in the small Reynolds number limit, where Coriolis and other inertial effects are negligible [5]. For the inclusion of such effects into the rotating Hele-Shaw problem, we refer the reader to Refs. [7,8,10].

From Eq. (1) and the incompressibility condition $\nabla\cdot\mathbf{v}_j = 0$, it can be verified that the velocity potential $\phi_j$ ($\mathbf{v}_j = -\nabla\phi_j$) obeys Laplace's equation $\nabla^2\phi_j = 0$. The problem is then specified by two boundary conditions at the interface

$$p_1 - p_2 = \sigma(\mathcal{K})\mathcal{K} \tag{2}$$

and

$$\mathbf{n}\cdot\nabla\phi_1 = \mathbf{n}\cdot\nabla\phi_2. \tag{3}$$

Equation (2) is a modified version of the usual Young-Laplace pressure jump at the interface [31] with $\mathcal{K} = \kappa + \kappa_\perp$, where $\kappa$ denotes the spatially varying interfacial curvature in the plane of the Hele-Shaw cell, and $\kappa_\perp = \cos\theta_c/(b/2)$ is the constant curvature associated with the interface profile in the direction perpendicular to the Hele-Shaw plates, set by the static contact angle $\theta_c$ measured between the plates and the curved meniscus. In Eq. (2) note the presence of a curvature-dependent surface tension given by

$$\sigma(\mathcal{K}) = \sigma_0 + \beta\mathcal{K}, \tag{4}$$

where the control parameter $\beta$ can be positive, negative, or zero, and $\sigma_0$ is the surface tension when $\beta = 0$ [32,33]. The possible physical mechanisms involved with this particular functional form of the variable interfacial tension are related to the addition of surfactants or polymers at the fluid-fluid interface, or at the cell walls. These issues have been thoroughly discussed in Refs. [31–33].

Depending on the values of $\beta$ and $\theta_c$, the effective surface tension can be either reduced or increased when the interface bulges into the displaced fluid, altering the stability of the fluid-fluid interface. As in Refs. [27,29] we focus on the situation in which the displaced fluid is nonwetting ($\theta_c = \pi$). The second important boundary condition [Eq. (3)], known as the kinematic boundary condition, states that the normal components of each fluid's velocity are continuous at the interface, with $\mathbf{n}$ representing the interface unit normal vector.

At this point we stress that the coupling between the curvature-dependent surface tension $\sigma(\mathcal{K})$ and the three-dimensional (3D) term represented by $\kappa_\perp$ plays a fundamental role in allowing a proper manipulation of the centrifugal fingering instability. If the surface tension does not depend on the curvature ($\beta = 0$), since the 3D term is constant (its gradient is zero), it does not affect the motion of the interface. However, if $\beta \neq 0$ we have the coupling of $\beta$ and the spatially varying in-plane curvature $\kappa$ with the 3D term.

To obtain a mode-coupling differential equation for the interface evolution, we follow standard steps performed in previous weakly nonlinear studies in Hele-Shaw cells [31,35]: from the solution of Laplace's equation we define Fourier expansions for the velocity potentials. Then, we express $\phi_j$ in terms of the perturbation amplitudes $\zeta_n$ by considering condition (3). Substituting these relations and the modified pressure jump condition Eq. (2) into Eq. (1), always keeping terms up to second order in $\zeta$, and Fourier transforming, we find the *dimensionless* equation of motion for the perturbation amplitudes (for $n \neq 0$),

$$\dot{\zeta}_n = \lambda(n)\zeta_n + \sum_{n'\neq 0}[F(n,n')\zeta_{n'}\zeta_{n-n'} + G(n,n')\dot{\zeta}_{n'}\zeta_{n-n'}], \tag{5}$$

where the overdot denotes total time derivative, and

$$\lambda(n) = |n|\left\{\mathrm{sgn}(U) - S(n^2-1)\left[1 + 2\mathfrak{B}\left(1 + \frac{2\cos\theta_c}{b}\right)\right]\right\} \tag{6}$$

is the (time-independent) linear growth rate. The parameter

$$S = \frac{\sigma_0}{R^3\Omega^2|\rho_1 - \rho_2|} \tag{7}$$

represents the ratio of capillary to centrifugal forces, while

$$\mathfrak{B} = \frac{\beta}{\sigma_0 R} \tag{8}$$

measures the action of curvature-dependent surface-tension effects. The sgn function equals $\pm 1$ according to the sign of its argument.

The second-order mode-coupling terms are given by

$$F(n,n') = |n|\left\{\frac{1}{2}\mathrm{sgn}(U) - S\left(1+4\mathfrak{B}\frac{\cos\theta_c}{b}\right)\left[1-\frac{n'}{2}(3n'+n)\right] - S\mathfrak{B}[3-n'(5n'+n)+n'^2(n-n')^2]\right\} \quad (9)$$

and

$$G(n,n') = A|n|[1-\mathrm{sgn}(nn')]-1, \quad (10)$$

where $A=(\eta_2-\eta_1)/(\eta_2+\eta_1)$ is the viscosity contrast. In Eq. (5) lengths are rescaled by $R$, and time by $R/U$, where $U=[b^2R(\rho_1-\rho_2)\Omega^2]/[12(\eta_1+\eta_2)]$ is a characteristic velocity. From this point on, we will be dealing with the dimensionless version of the governing equations.

The linear growth rate (6) provides relevant information about the linear stability of the interface, and the nonlinear terms (9) and (10) offer key analytical insights into the response of finger competition events to the action of the variable interfacial tension at the weakly nonlinear regime. As pointed out at the beginning of this section, recall that in this work we focus on the centrifugally unstable situation in which $\mathrm{sgn}(U)=1$, $A=-1$, and $\theta_c=\pi$. These are the most common conditions present in existing experiments in rotating Hele-Shaw cells. Moreover, these are also the conditions of important technological applications [12–16] where control of centrifugal fingering could be needed. We emphasize that the values we take for our dimensionless parameters are consistent with typical physical quantities used in real experiments for rotating Hele-Shaw flows [4,5,9].

## III. FINGERING CONTROL: LINEAR AND NONLINEAR REGIMES

As mentioned earlier in this work, our main goal is to use the curvature-dependent surface-tension approach to stabilize usually unstable flows in rotating Hele-Shaw cells. First, in Sec. III A we try to extract useful information regarding control of centrifugally driven instabilities at purely linear, early time stages of the interface evolution. Then, in Sec. III B we test the robustness of the control strategy verified at the linear level, turning our attention to the weakly nonlinear regime. At the nonlinear level, we can examine how the variable interfacial tension acts on the typical finger competition mechanism which takes place in rotating Hele-Shaw flows.

### A. Linear behavior

We begin our discussion by examining the origin of the terms in the linear growth rate expression [Eq. (6)]. Since we concentrate on the situation where $\mathrm{sgn}(U)=1$, it is clear that the centrifugal term does act to destabilize the system. On the other hand, the second term proportional to $S(n^2-1)$ is related to the surface-tension contributions: the first term on the square bracket is associated to the surface tension connected to the in-plane curvature $\kappa$, and plays a stabilizing role. The term proportional to the variable surface-tension parameter $\mathfrak{B}$ presents the contribution due to the transverse interfacial curvature $\kappa_\perp$ involving the contact angle. Recall that Hele-Shaw flows consider a high aspect ratio situation where $b\ll 1$ so that the contact angle term is indeed the dominant one. Finally, notice that since here we consider that $\theta_c=\pi$, $\mathfrak{B}$ must be negative in order to stabilize the interface. Of course, if $\mathfrak{B}>0$ the interface would be further destabilized, but this is not the effect in which we are currently interested.

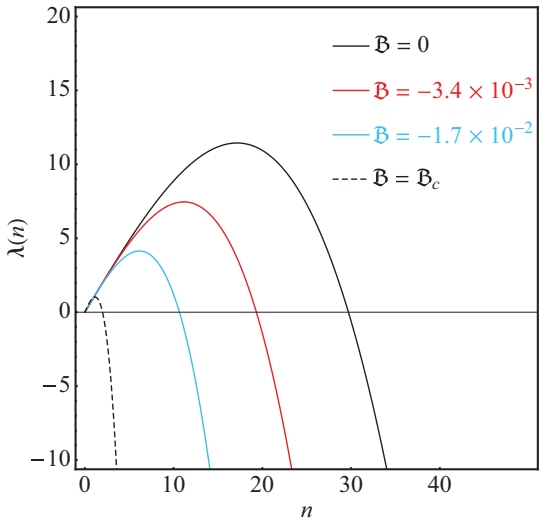


FIG. 2. (Color online) Inhibition of centrifugal fingering at the linear level. Linear growth rate $\lambda(n)$ as a function of mode number $n$ for different values of $\mathfrak{B}$. The typical number of interfacial fingers, given by the maximum of the curves ($n_{\max}$), drops successively ($n_{\max}\approx 17,11,6$, and 1) as the magnitude of the variable interfacial tension parameter $\mathfrak{B}$ is increased.

The role of $\mathfrak{B}$ in controlling the instability at the linear level is illustrated in Fig. 2. This figure plots the linear growth rate (6) as a function of mode number $n$ for different values of the variable surface-tension parameter $\mathfrak{B}$: 0, $-3.4\times10^{-3}$, $-1.7\times10^{-2}$, and $\mathfrak{B}_c$, where $\mathfrak{B}_c$ denotes the critical value for which all modes $n>1$ become stable [obtained by setting $\lambda(n)=0$]

$$\mathfrak{B}_c = \frac{1}{2\left(1+\frac{2\cos\theta_c}{b}\right)}\left[\frac{\mathrm{sgn}(U)}{S(n^2-1)}-1\right]. \quad (11)$$

Figure 2 is plotted by considering the following typical values of $S$ and $b$: $S=1.14\times10^{-3}$ and $b=10^{-2}$. As a matter of fact, these characteristic parameter values will also be used to plot the remaining figures appearing in this work.

By inspecting Fig. 2 it is clear that the system is unstable when $\mathfrak{B}=0$: there is a large band of unstable modes, for which $\lambda(n)>0$. Note that the maximum of the curve represents the mode of largest growth $n_{\max}$ [obtained by setting $d\lambda/dn=0$]. For $\mathfrak{B}=0$ we find that $n_{\max}\approx 17$. This number represents the typical number of fingers that emerges at the rotating interface in the linear regime. Moreover, Fig. 2 indicates that for $\mathfrak{B}=-3.4\times10^{-3}$ the interface becomes more stable compared with the $\mathfrak{B}=0$ case: the band of unstable modes is reduced, the growth rate magnitude is decreased, and the number of fingers drops (now $n_{\max}\approx 11$).

We can also see that by further increasing the magnitude of $\mathfrak{B}$ one could stabilize the system quite significantly, making $n_{\max}$ drop to one when $\mathfrak{B} = \mathfrak{B}_c$ [Eq. (11)].

In order to suppress any interfacial instability it would suffice to consider the case $n \geqslant 2$. The mode $n = 0$ that corresponds to a uniform expansion of the circle is marginal [i.e., $\lambda(n = 0) = 0$] for all values of $\mathfrak{B}$. Note that mode $n = 1$ does not introduce any interfacial deformations. In fact, it corresponds to a global off-center shift of the circle. So, it preserves circular shape but can be unstable in the sense that it can lead to droplet translation.

### B. Weakly nonlinear stage

Although it is encouraging to be able to verify that at the linear level one could use the parameter $\mathfrak{B}$ to control the degree of centrifugal fingering, rigorously it does not guarantee that such a controlling strategy will be really effective during nonlinear stages of the interface evolution. Additionally, the typical finger competition phenomenon verified in rotating Hele-Shaw flows is an intrinsically nonlinear effect and cannot be properly addressed by purely linear analysis [6,36–38]. Therefore, to check the linear predictions discussed in Sec. III A, and to elucidate key effects related to finger competition in rotating Hele-Shaw flow in the presence of a variable interfacial tension, we proceed by analyzing the weakly nonlinear dynamics of the system. This is done by concentrating our attention on the role played by the parameter $\mathfrak{B}$ in possibly controlling finger competition events, and ultimately leading to interface stabilization.

Now the mode-coupling equation (5) is utilized in its entirety to study the onset of nonlinear pattern formation through the coupling of a small number of modes. To simplify our discussion it is convenient to rewrite the complex net perturbation in terms of cosine and sine modes,

$$\zeta(\theta,t) = \zeta_0 + \sum_{n=1}^{\infty} [a_n(t)\cos(n\theta) + b_n(t)\sin(n\theta)], \quad (12)$$

where $a_n = \zeta_n + \zeta_{-n}$ and $b_n = i(\zeta_n - \zeta_{-n})$ are real valued. Without loss of generality, for the remainder of this work, we choose the phase of the fundamental mode so that $a_n > 0$ and $b_n = 0$. We follow Ref. [35] and consider finger length variability as a measure of the competition among fingers. Within our approach the finger competition mechanism can be described by the influence of a fundamental mode $n$, assuming $n$ is even, on the growth of its subharmonic mode $n/2$. By using Eqs. (5)–(10) the equations of motion for the subharmonic mode can be written as

$$\dot{a}_{n/2} = \{\lambda(n/2) + \mathcal{C}(n)a_n\}a_{n/2}, \quad (13)$$

$$\dot{b}_{n/2} = \{\lambda(n/2) - \mathcal{C}(n)a_n\}b_{n/2}, \quad (14)$$

where the finger competition function is given by

$$\mathcal{C}(n) = \frac{1}{2}\left[C\left(\frac{n}{2},-\frac{n}{2}\right) + C\left(\frac{n}{2},n\right)\right] \quad (15)$$

and

$$C(n,n') = F(n,n') + \lambda(n')G(n,n'). \quad (16)$$

From Eqs. (13) and (14) we verify that a negative $\mathcal{C}(n)$ increases the growth of the sine subharmonic $b_{n/2}$, while inhibiting growth of its cosine subharmonic $a_{n/2}$. The result is an increased variability among the lengths of fingers of the outer fluid penetrating into the inner one. This effect describes the competition of inward fingers. Note that our finger competition mechanism determines the preferred direction for finger growth and finger length variability. So, when

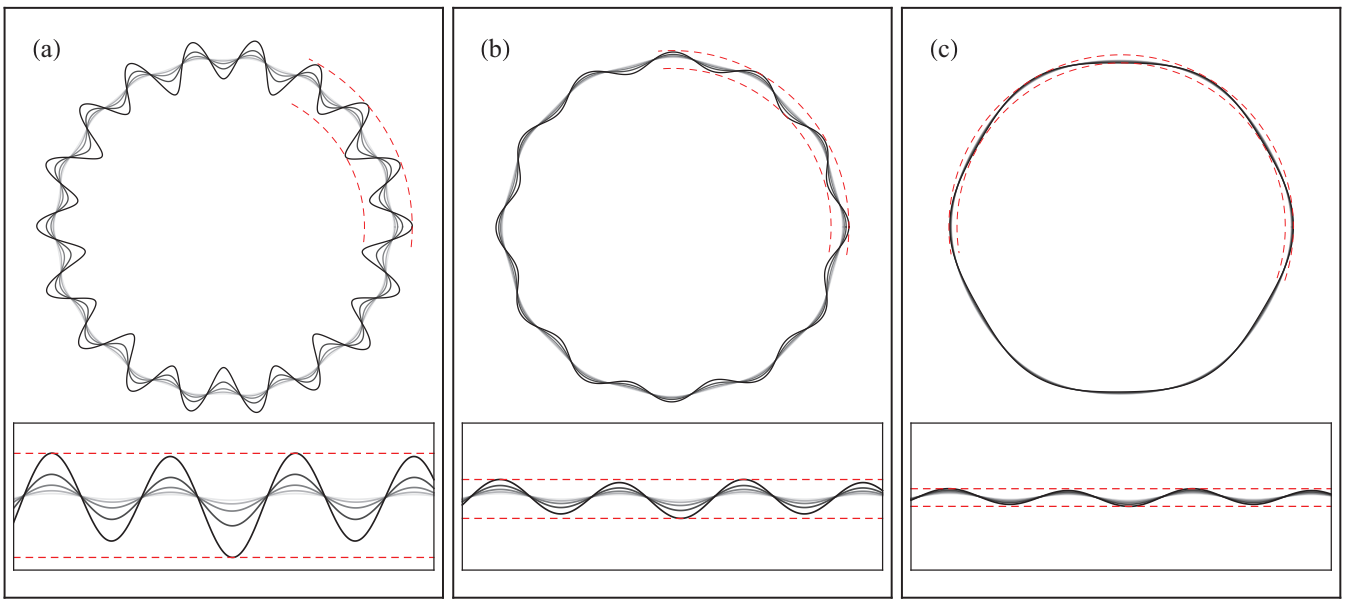


FIG. 3. (Color online) Inhibition of centrifugal fingering at the weakly nonlinear level. Snapshots of the evolving interface, plotted at equal time intervals for the interaction of the fundamental mode, and its subharmonic. Different values of the variable interfacial tension parameter $\mathfrak{B}$ are used: (a) 0, (b) $-3.4 \times 10^{-3}$, and (c) $-1.7 \times 10^{-2}$. The dashed curves are added to better guide the eye regarding finger competition. The insets show close-up views of the regions delimited by the dashed curves. Darker colors mean later times.

$\mathcal{C}(n) < 0$, even though there exists finger competition in both directions (inward and outward), the competition among inward moving fingers is much stronger than the competition among outward moving fingers. Reversing the sign of $\mathcal{C}(n)$ would exactly reverse these conclusions, such that modes $a_{n/2}$ would be favored over modes $b_{n/2}$. In this case, competition of the outward moving fingers of the inner fluid would have preferential growth.

For the typical rotating Hele-Shaw flow experimental parameters used in Refs. [4,5,9] we have found that $\mathcal{C}(n) < 0$ indicating a restrained growth of cosine subharmonic modes $a_{n/2}$, accompanied by a simultaneous increased growth of sine subharmonic modes $b_{n/2}$. These findings are illustrated in Fig. 3, which plots the time evolution of the rotating fluid-fluid interface for three different values of $\mathfrak{B}$: 0, $-3.4 \times 10^{-3}$, and $-1.7 \times 10^{-2}$. The interfaces shown in this figure are calculated with the help of Eq. (12) and consider the weakly nonlinear interplay of two wave numbers, namely the fundamental $n = n^*$, where $n^*$ is the nearest even integer to $n_{\max}$ and its subharmonic $n/2$. We take the initial amplitudes as $a_{n/2}(0) = b_{n/2}(0) = 1/750$ and $a_n(0) = 1/130$. In addition, the interfaces are plotted for $0 \leqslant t \leqslant 0.247$, at equal time intervals $\Delta t = 0.062$. As in Fig. 2, $S = 1.14 \times 10^{-3}$ and $b = 10^{-2}$. These parameters are also utilized to plot Fig. 4.

By examining Fig. 3(a) for $\mathfrak{B} = 0$ it is evident that the inward moving fingers of the outer fluid present different lengths, indicating the presence of finger competition. The inset of Fig. 3(a) shows a close-up view of part of the fingers, where competition among inward moving fingers can be clearly verified: some inward moving fingers touch the inner dashed line, while other inward moving fingers do not. On the other hand, the fingers of the inner fluid pointing outward have nearly similar sizes, confirming the prediction that competition among these fingers is repressed. So, the fact is that when the surface tension is constant, one does observe a finger competition phenomenon among inward moving fingers.

A different kind of behavior is revealed in Fig. 3(b) for $\mathfrak{B} = -3.4 \times 10^{-3}$: the action of the variable interfacial tension not only reduces the number of fingers, but also decreases the competition of the inward moving fingers. By inspecting the inset of Fig. 3(b) we see that both neighboring inward moving fingers are very close to the inner dashed line, indicating weaker competition. Finally, by increasing the magnitude of $\mathfrak{B}$ even further [in Fig. 3(c) $\mathfrak{B} = -1.7 \times 10^{-2}$] we obtain a much more stabilized fluid-fluid interface in which finger competition events are hardly observable, as illustrated by the inset of Fig. 3(c). This supports the idea that the variable interfacial tension approach is effective in suppressing finger competition events, and interface disturbances in general, also at weakly nonlinear stages of the dynamics.

In order to reinforce the visual illustration of the restrained finger competition for larger $\mathfrak{B}$ discussed in Fig. 3, we go ahead and analyze this issue more quantitatively in Fig. 4. The evaluation of finger competition is done by the quantity

$$\Delta\mathfrak{R} = |\mathfrak{R}_i - \mathfrak{R}_{i+1}|, \tag{17}$$

which expresses the absolute value of the difference between the interfacial positions for consecutive *inward* moving fingers $i$ and $i + 1$, where $\mathfrak{R}_i$ is the radial position of the tip of an $i$th inward moving finger and $\mathfrak{R}_{i+1}$ is the equivalent position of the neighboring inward moving finger [or the $(i + 1)$th finger]. These geometric concepts are sketched in Fig. 4(a). Note that $\Delta\mathfrak{R}$ provides a convenient quantitative measure of the finger length variability or, equivalently, of the finger competition events among inward moving fingers.

Useful information about the time evolution of the finger competition behavior in our system can then be obtained by analyzing Fig. 4(b) that plots $\Delta\mathfrak{R}$ as a function of time. Note that the curves for $\mathfrak{B} \neq 0$ are located below the one for $\mathfrak{B} = 0$

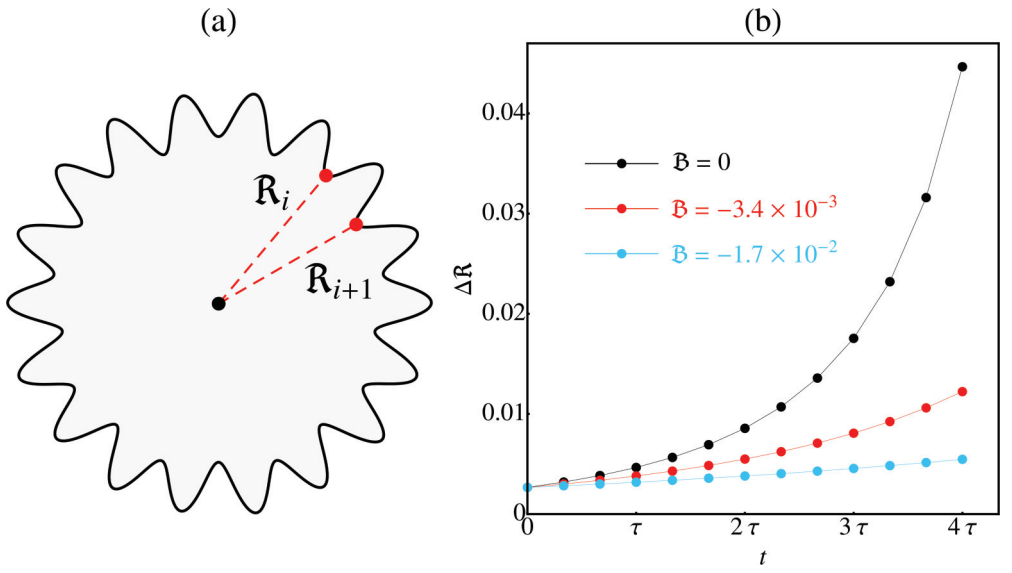


FIG. 4. (Color online) Refers to the patterns illustrated in Fig. 3, and uses the same physical parameters. Difference between the interface positions of the fingertips for consecutive inward moving fingers of the outer fluid $\Delta\mathfrak{R}$ [see Eq. (17) and Fig. 4(a)] as a function of time, for different values of $\mathfrak{B}$ as plotted in Fig. 4(b). One readily observes that finger competition is decreased by the use of variable interfacial tension of increasingly larger magnitude. Here $\tau = 15\Delta t$, where $\Delta t$ is the time interval used in Fig. 3.

expressing that finger competition decreases as the magnitude of $\mathfrak{B}$ is increased. This demonstrates in a quantitative fashion that finger competition is significantly affected by the variable interfacial tension parameter $\mathfrak{B}$. This makes it appropriate to properly tune and control centrifugal fingering in general, and nonlinear finger competition events in particular.

## IV. CONCLUSION

In this work, we revisited the rotating Hele-Shaw flow problem, and investigated the effect of a curvature-dependent interfacial tension on the stability properties of the fluid-fluid interface. This was done by performing a weakly nonlinear analysis of the rotating flow situation. It enabled us to verify the effectiveness of the variable interfacial tension approach in controlling centrifugal fingering both at purely linear stages of the dynamics, as well as at the onset of nonlinearities. In particular, we showed that nonlinear finger competition events can be systematically suppressed, yielding subsequent interface stabilization. This work offers an additional contribution to the growing body of recent studies in the literature addressing a number of different strategies targeting the control of interfacial instabilities in confined Hele-Shaw geometries [22–31].

## ACKNOWLEDGMENTS

We thank CNPq for financial support through the program "Instituto Nacional de Ciência e Tecnologia de Fluidos Complexos (INCT-FCx)" and FACEPE through PRONEM Project No. APQ-1415-1.05/10.

[1] P. G. Saffman and G. I. Taylor, Proc. R. Soc. A **245**, 312 (1958).
[2] G. M. Homsy, Annu. Rev. Fluid Mech. **19**, 271 (1987); K. V. McCloud and J. V. Maher, Phys. Rep. **260**, 139 (1995); J. Casademunt, Chaos **14**, 809 (2004).
[3] L. W. Schwartz, Phys. Fluids A **1**, 167 (1989).
[4] Ll. Carrillo, F. X. Magdaleno, J. Casademunt, and J. Ortín, Phys. Rev. E **54**, 6260 (1996).
[5] E. Alvarez-Lacalle, J. Ortín, and J. Casademunt, Phys. Fluids **16**, 908 (2004).
[6] J. A. Miranda and E. Alvarez-Lacalle, Phys. Rev. E **72**, 026306 (2005).
[7] S. L. Waters and L. J. Cummings, Phys. Fluids **17**, 048101 (2005).
[8] A. Abidate, S. Aniss, O. Caballina, and M. Souhar, Phys. Rev. E **75**, 046307 (2007).
[9] R. Folch, E. Alvarez-Lacalle, J. Ortín, and J. Casademunt, Phys. Rev. E **80**, 056305 (2009).
[10] E. O. Dias and J. A. Miranda, Phys. Rev. E **83**, 046311 (2011).
[11] J. Casademunt, Eur. Phys. J. Plus **126**, 94 (2011), and references therein.
[12] S. L. Waters, L. J. Cummings, K. M. Shakesheff, and F. R. A. J. Rose, IMA J. Math. Med. Biol. **23**, 311 (2006).
[13] M. A. Fardin, M. O. Rossier, P. Rangamani, P. D. Avigan, N. C. Gauthier, W. Vonnegut, A. Mathur, J. Hone, R. Iyengar, and M. P. Sheetz, Soft Matter **6**, 4788 (2010).
[14] C. Blanch-Mercader and J. Casademunt, Phys. Rev. Lett. **110**, 078102 (2013).
[15] L. W. Schwartz and R. V. Roy, Phys. Fluids **16**, 569 (2004).
[16] K. E. Holloway, P. Habdas, N. Semsarillar, K. Burfitt, and J. R. de Bruyn, Phys. Rev. E **75**, 046308 (2007).
[17] D. G. Crowdy, Q. Appl. Math. **60**(1), 11 (2002).
[18] E. S. G. Leandro, R. M. Oliveira, and J. A. Miranda, Physica D **237**, 652 (2008).
[19] R. López, Appl. Math. Lett. **22**, 860 (2009).
[20] N. R. McDonald, Eur. J. Appl. Math. **22**, 517 (2011).
[21] M. Ehrnström, J. Escher, and B. V. Matioc, J. Math. Fluid Mech. **13**, 271 (2011).
[22] S. W. Li, J. S. Lowengrub, J. Fontana, and P. Palffy-Muhoray, Phys. Rev. Lett. **102**, 174501 (2009).
[23] B. Jha, L. Cueto-Felgueroso, and R. Juanes, Phys. Rev. Lett. **106**, 194502 (2011).
[24] E. O. Dias, E. Alvarez-Lacalle, M. S. Carvalho, and J. A. Miranda, Phys. Rev. Lett. **109**, 144502 (2012).
[25] D. Pihler-Puzović, P. Illien, M. Heil, and A. Juel, Phys. Rev. Lett. **108**, 074502 (2012).
[26] D. Pihler-Puzović, R. Périllat, M. Russell, A. Juel, and M. Heil, J. Fluid Mech. **731**, 162 (2013).
[27] T. T. Al-Housseiny, P. A. Tsai, and H. A. Stone, Nature Phys. **8**, 747 (2012).
[28] R. M. Wilson, Phys. Today **65**(10), 15 (2012).
[29] T. T. Al-Housseiny, I. C. Christov, and H. A. Stone, Phys. Rev. Lett. **111**, 034502 (2013).
[30] T. T. Al-Housseiny and H. A. Stone, Phys. Fluids **25**, 092102 (2013).
[31] F. M. Rocha and J. A. Miranda, Phys. Rev. E **87**, 013017 (2013).
[32] H. Guo, D. C. Hong, and D. A. Kurtze, Phys. Rev. Lett. **69**, 1520 (1992).
[33] H. Guo, D. C. Hong, and D. A. Kurtze, Phys. Rev. E **51**, 4469 (1995).
[34] A. similar variable interfacial tension approach is utilized in crystal theory where a dependence of the surface tension on the curvature is introduced to smooth out the crystal corners. See, e.g., A. A. Wheeler, Proc. R. Soc. A **462**, 3363 (2006).
[35] J. A. Miranda and M. Widom, Physica D **120**, 315 (1998).
[36] H. Gadêlha and J. A. Miranda, Phys. Rev. E **70**, 066308 (2004).
[37] C.-Y. Chen, C.-H. Chen, and J. A. Miranda, Phys. Rev. E **73**, 046306 (2006).
[38] C.-Y. Chen, Y. S. Huang, and J. A. Miranda, Phys. Rev. E **84**, 046302 (2011).